Broadband Dielectric Resonator Antenna With Metal Coating

Tze-Hsuan Chang, *Student Member, IEEE*, and Jean-Fu Kiang, *Member, IEEE*

***Abstract*—A broadband dielectric resonator (DR) antenna is proposed, which consists of a rectangular DR coated with metal on three sides and placed on a ground plane. The structure is analyzed by modelling the dielectric-air interface as perfect magnetic conductor (PMC). A coplanar waveguide (CPW) with terminating slots is used to feed the antenna. Measurement results exhibit a wide bandwidth of about 47% over which the E_θ pattern on the horizontal plane is nearly omnidirectional. The 10-dB bandwidth of this broadband DR monopole covers 4.2–6.8 GHz. Hence, it can be used for WLAN 802.11a applications.**

***Index Terms*—Dielectric resonator (DR) antenna, monopole antenna.**

I. Introduction

The prevalence of wireless communication demands broadband antennas which can be embedded within a handset to provide versatile applications. Since it is difficult to obtain wide impedance bandwidth with single resonant antenna, multiple antennas with different operating frequencies have been integrated to satisfy the bandwidth requirement [1], [2].

High-permittivity dielectric material has been used in microwave circuits such as filters or oscillators [3]. In order to facilitate the design of dielectric resonator, a heuristic approach that models the dielectric-air interface as a perfect magnetic wall was proposed to predict the resonant frequencies of cylindrical resonators in 1965 [4]. Since 1983, dielectric resonators have been designed as antenna elements by exciting different modes of DR using conventional feeding mechanisms [5].

A DR antenna exhibits a broader bandwidth if its Q factor is lower. In [6], a notched rectangular DR antenna with a low Q factor is proposed. By lifting a DR above the ground plane, its Q factor can be effectively reduced [7]. The bandwidth of DR can also be increased by modifying its geometry. For example, a truncated tetrahedral DR with its narrow base attached to the ground reaches an impedance bandwidth of 40% [8]. A split conical DR with split side attached to the ground can reach a bandwidth of 50% [9].

High-permittivity material can be used to reduce the size of DR at the expense of bandwidth reduction. However, DRs with larger aspect ratio has been used to reduce the Q factor and hence obtain a wider impedance bandwidth [10], [11].

Multiple DRs with close resonant frequencies can exhibit broadband characteristics by coupling their resonant modes. For example, two cylindrical DRs can be stacked to couple their $\mathrm{HEM}_{11\delta}$ modes [1]. In [2], two rectangular DRs with different sizes are placed at proximity, leaving a slot to couple their TE_{111}^y modes.

The bandwidth of DR antenna can also be extended by attaching additional parasitic elements to incur another resonance. In [12], two metal strips are attached to the top of a DR to incur additional resonance close to that of the DR. The inductance of the metal strip and the capacitance between the strip and the ground plane form an LC tank which can be coupled to the DR resonant mode to exhibit a wider bandwidth.

The impedance bandwidth of DR antennas can be further increased by modifying their feeding structures. In [13], a coupling slot is proposed to excite the DR. The resonant modes of slot and DR are coupled to increase the antenna bandwidth.

In [14], a patch resonant mode and a dielectric resonant mode are coupled to increase the DR antenna bandwidth. The signal is fed from the microstrip feed line, through the slot on the ground plane and the slot on the patch, to the DR. In [15], a DR is attached to a circular slot and an eccentric ring slot to achieve a broad bandwidth. A grounded metal plate placed in a plane of symmetry of the electric field distribution can reduce the DR size by half without perturbing the original field distribution. In [16], a rectangular DR integrated with an inverted L-plate antenna is proposed. The DR not only serves as a radiator but also serves as a feeding element for the L-plate.

Typical bandwidth of a rectangular DR antenna is about 6–10%, which can be increased to more than 10% by using lower-permittivity dielectric at the cost of increasing the DR size. Stacking DRs of different sizes or using parasitic DRs can further increase the impedance bandwidth to more than 20% [1], [2]. The former incurs a higher antenna profile, while the latter occupies larger space. Stacking DRs of different permittivities can achieve well coupling to microstrip line and a wider bandwidth of 40% simultaneously. However, the antenna complexity increases. Conical or truncated conical DR can provide more than 50% of impedance bandwidth, but the radiation pattern varies over the band due to the presence of higher-order modes [9].

In this work, a broadband dielectric resonator antenna with a nearly-omnidirectional radiation pattern is proposed. The dielectric resonator is partially coated with metal on its surface, which can be modeled as a cavity having perfect electric conductor (PEC) and perfect magnetic conductor (PMC) walls on

Manuscript received October 24, 2006. This work was sponsored by the National Science Council, Taiwan, ROC, under contract NSC 93-2213-E-002-034.

The authors are with the Department of Electrical Engineering and the Graduate Institute of Communication Engineering, National Taiwan University, Taipei, Taiwan (e-mail: jfkiang@cc.ee.ntu.edu.tw).

Color versions of one or more of the figures in this paper are available online at http://ieeexplore.ieee.org.

Digital Object Identifier 10.1109/TAP.2007.895582

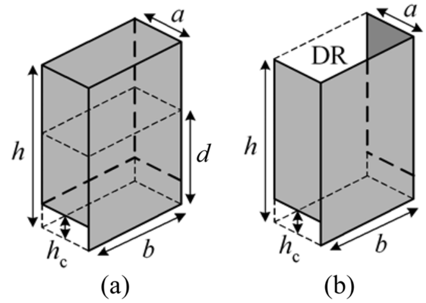

Fig. 1. DR with metal coating on the bottom and on the other: (a) five sides and (b) three sides, gap of height h_c is open near the bottom, metal coating is marked by gray shade.

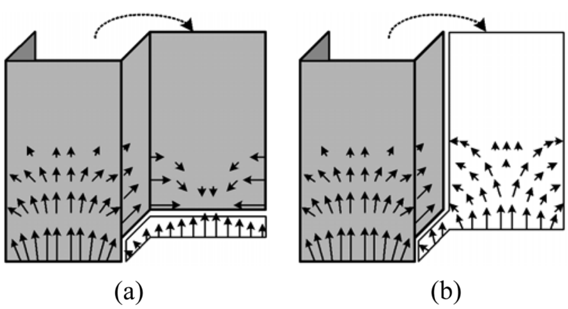

Fig. 2. Current distribution on metal coating (gray surface), and electric field distribution on DR surface (white surface), corresponding to the DR in Figs. 1(a) and (b), respectively.

TABLE I
EFFECT OF STRUCTURE DIMENSIONS ON THE RESONANT FREQUENCY (f_r)

h (mm)	6	8	10	12	14	
f_r (GHz)	6.5	6.49	6.5	6.47	6.49	
b (mm)	3	3.5	4	4.5	5	
f_r (GHz)	7.13	6.83	6.41	6.15	5.79	
a (mm)	1.5	1.7	1.9	2.1	2.3	2.5
f_r (GHz)	7.59	7.13	6.67	6.27	5.87	5.53
d (mm)	1	2	3	4	8	12
f_r (GHz)	8.09	6.7	6.54	6.52	6.46	6.47
h_c (mm)	0.2	0.5	0.8	1.4	1.7	2
f_r (GHz)	5.68	6.09	6.37	6.59	6.75	6.91

Default parameter (mm): $a = 2$, $b = 4$, $d = 12$, $h = 12$, $h_c = 1$, DR is coated on five sides and grounded as in Fig. 1(a).

(a)

$h = d$ (mm)	10	11	12	13	14	
f_r (GHz)	6.05	6.02	6.08	6.04	6.07	
b (mm)	5	5.5	6	6.5	7	
f_r (GHz)	6.07	6.05	6.07	6.05	5.99	
a (mm)	2.5	2.7	2.9	3.1	3.3	3.5
f_r (GHz)	7.14	6.6	6.17	5.84	5.49	5.19
h_c (mm)	0.2	0.5	0.8	1.4	1.7	2
f_r (GHz)	5.68	6.09	6.37	6.59	6.75	6.91

Default parameters (mm): $a = 3$, $b = 6$, $d = h = 12$, $h_c = 1$, DR is coated on three sides and grounded as in Fig. 1(b).

(b)

different portions of the surface. The resonant modes of the DR are investigated. The electric field and the current distributions of these modes are carefully studied to understand their relation to the radiation patterns. The metal coating is also fed as a monopole. The input impedance can be matched by adjusting the DR position and the slot length, and broad bandwidth is achieved by coupling the resonant modes of the metal-coated DR and the monopole.

II. RESONANT MODES OF COATED DR

Fig. 1(a) shows a rectangular dielectric resonator partially coated with metal, and a small gap of height h_c is open near the bottom of the dielectric resonator. Since the permittivity of the dielectric is much higher than that of the air, the dielectric-air interface can be approximated as a PMC boundary, and the metal coating is treated as a PEC boundary. Hence, the structure is a cavity with PEC and PMC on different portions of the surface, filled with high-permittivity dielectric.

The current and the electric field distributions of the fundamental mode are plotted in Fig. 2(a). The fields and the currents concentrate near the bottom of the dielectric. The electric field across the gap is mainly parallel to the PMC surface. The current flows vertically from the bottom, changes direction on the metal coating, and ends on the opposite side.

The effects of varying parameters are summarized in Table I. It is observed that the resonant frequency is significantly affected by the DR dimensions a and b, and is less affected by the metal height h, since the fields concentrate near the bottom. The effect of decreasing the DR height d while keeping h constant has also been considered. The height d has significant effect on the resonant frequency only when d is comparable to h_c.

Fig. 2(a) shows that the current of the fundamental mode on the back coating has strong horizontal component, which generates electric field with horizontal polarization on the xy-plane. Hence, the back coating is removed to reduce the horizontal current, as shown in Fig. 1(b). Fig. 2(b) shows the current and the electric field distributions on the metal coating and the DR surface, respectively. The current distribution is similar to that in Fig. 2(a). The electric field starts from the bottom vertically, gradually decreases and bends to terminate at the metal coating. The effects of varying parameters are also summarized in Table I. Compared to that in Fig. 2(a), the width b now has little effect on the resonant frequency.

III. MONOPOLE MODE OF METAL COATING

Place the DR with metal coating as shown in Fig. 1(b) on a ground plane as shown in Fig. 4(a). The metal coating is connected to coplanar waveguide (CPW) signal line to form a monopole antenna, and its resonant frequency is increased as its height is decreased. Fig. 3 shows that the current flows mainly vertically, having a maximum near the ground plane. The current gradually decreases and vanishes at the top. The electric field starts from the ground plane, flows vertically inside the DR, bends and terminates at the coating. Both the current and the electric field have dominant vertical component, which generates strong vertical polarization on the xy-plane. Since the coating width is comparable to its height, the current has a small amount of horizontal component which generates the horizontal polarization on the xy plane.

IV. ANTENNA PROPERTIES

Fig. 4(a) shows the configuration of the proposed DR antenna. The DR with three-side metal coating shown in Fig. 1(b)

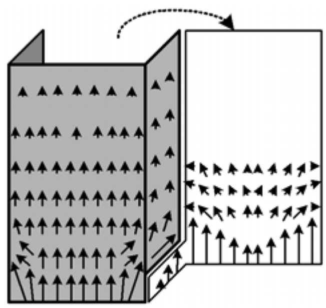

Fig. 3. Current and electric field distributions of the monopole mode on metal coating (gray surface) and DR surface (white surface), respectively.

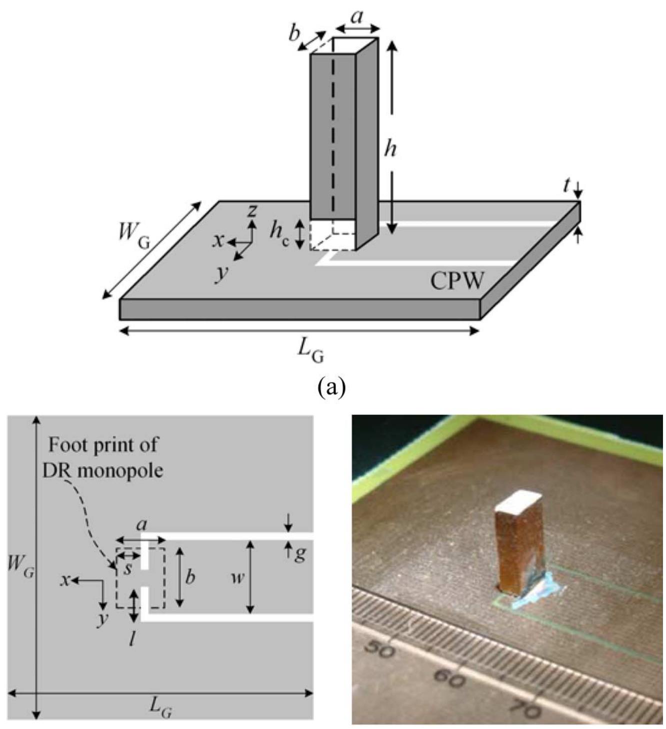

(a) (b) (c)

Fig. 4. (a) Configuration of DR-monopole antenna with feeding structure, (b) layout of feeding structure, and (c) photograph.

is placed on the ground plane, the metal coating is connected to the signal line of the CPW to excite the monopole mode, and a pair of open-circuited slots at the end of the CPW are used to excite the DR mode.

Fig. 4(b) shows the layout of the feeding structure, and Fig. 4(c) shows the photograph of the DR-monopole antenna. The DR is placed over the terminating slots of the CPW, and the length of the terminating slots is l. The size of ground plane is $L_G \times W_G$, and the thickness of the substrate is t. The width w and the gap g of the CPW are adjusted to obtain the characteristic impedance of 50 Ω.

By tuning the monopole height and the dimensions of DR, the resonant frequencies of the monopole and the fundamental mode of DR can be moved close to each other. By changing the lengths of the terminating slots l and the offset between the DR and the terminating slots s, good impedance matching can be

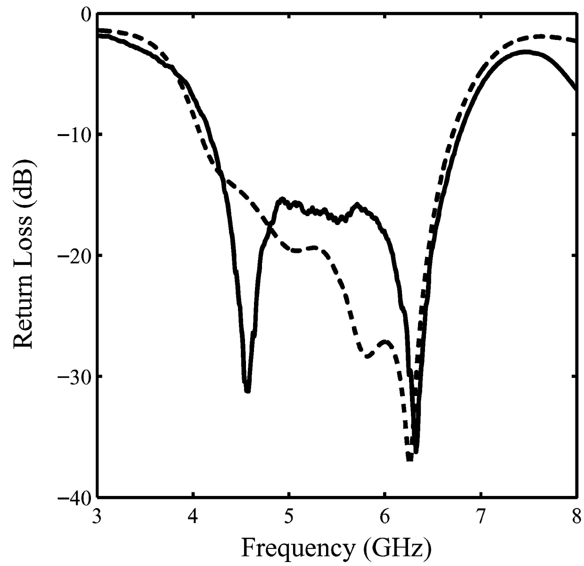

Fig. 5. Return loss of DR-monopole, $a = 3.3$ mm, $b = 5.6$ mm, $h = 12$ mm, $h_c = 0.5$ mm, $g = 0.5$ mm, $w = 10$ mm, $s = 0$ mm, $t = 0.6$ mm, $l = 5.25$ mm, $W_G = L_G = 70$ mm, —: measurement, - - -: simulation.

achieved. The broad impedance bandwidth is achieved by coupling the resonant bands of the monopole and the fundamental mode of DR with metal coating. Fig. 5 shows the return loss of the DR-monopole antenna, the measurement and the simulation results match reasonably well at the band edges. The 10-dB bandwidth is about 47.3% (4.2–6.8 GHz), which is wide enough to cover the IEEE 802.11a applications. Two nulls occurs at 4.56 GHz and 6.32 GHz, which are close to the resonant frequencies of the monopole and the fundamental mode of DR, respectively.

Fig. 6 shows the radiation patterns generated by the DR-monopole with coating on three sides and five sides, respectively. For frequency associated with the monopole mode, the DR-monopole with three-side coating has a more omnidirectional E_θ pattern on the xy-plane than that with five-side coating. The E_ϕ component with three-side coating is lower than that with five-side coating at $\phi = 75°$. For frequency associated with the fundamental mode of DR, the DR-monopole with three-side coating also has a more omnidirectional E_θ pattern on the xy-plane that with five-side coating. Hence, the DR with three-side coating is preferred.

Figs. 7 and 8 show the measurement and simulation radiation patterns at $f = 4.56$ GHz and $f = 6.32$ GHz, respectively. At $f = 4.56$ GHz, the E_θ pattern on the xy-plane is nearly omnidirectional, with the gain of about 1.2 dBi. The horizontal current exists on the side metal coating as shown in Fig. 3 and incurs E_ϕ component with multiple lobes. Hence, the E_ϕ component is only a few dB lower than the E_θ component in some directions. The E_θ pattern on the yz-plane is symmetric, and the maximum gain of 3.2 dBi occurs at $\theta = 44.6°$. The E_θ pattern on the xz-plane is asymmetric, and the maximum gain of 5.2 dBi occurs at $\theta = 33°$.

At $f = 6.32$ GHz, the horizontal current on the side coating as shown in Fig. 2(b) incurs E_ϕ components on the xy-plane with multiple lobes. The E_θ component on the xy-plane is

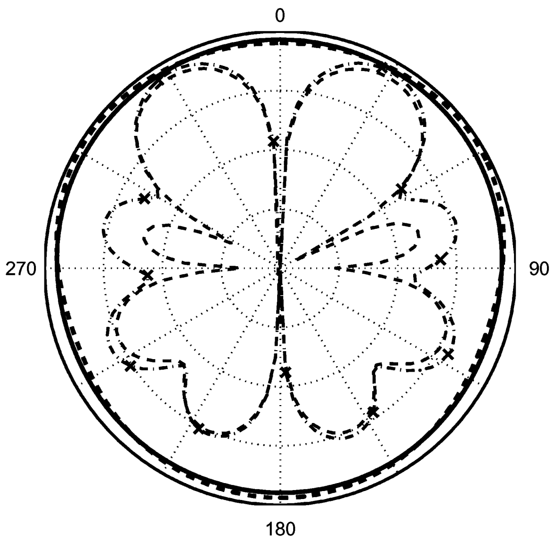

(a)

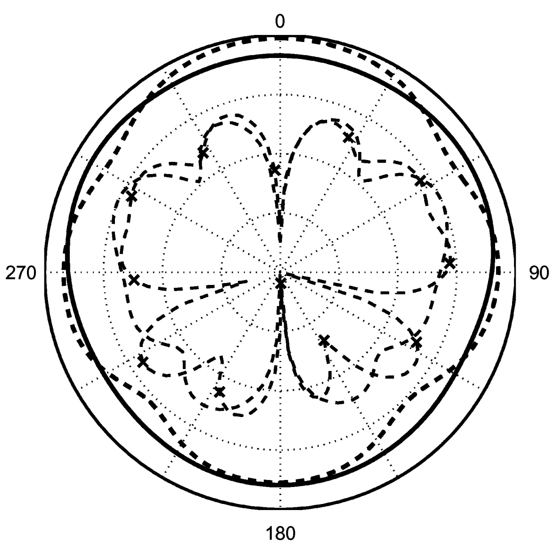

(b)

Fig. 6. Comparison of radiation patterns on xy-plane between DR with coating on three sides and five sides: (a) monople mode and (b) fundamental mode of DR, —: E_θ of DR with coating on three sides, - - -: E_θ of DR with coating on five sides, -·-: E_ϕ of DR with coating on three sides, -×-: E_ϕ of DR with coating on five sides, 10-dB per division on radials.

nearly omnidirectional with gain of 1.9 dBi. The E_θ pattern on the yz-plane is symmetric and has a maximum gain of 3.0 dBi at $\theta = 53°$, while that on the xz-plane is asymmetric with the maximum gain of 5.7 dBi at $\theta = 50°$.

The maximum of E_θ component on the xz- and the yz-planes is tilted from $\theta = 90°$ due to the finite size of ground plane. Hence, the antenna gain of vertical polarization is less than 2 dBi on the xy-plane. For WLAN applications, for example, this DR antenna can be placed on a desk with the z-axis pointing to zenith, providing a nearly omnidirectional radiation pattern with vertical polarization on the horizontal plane (xy-plane).

Fig. 9(a) shows the effect of antenna height h on the resonant frequency. When $h = 10$ mm, the resonant modes of the monopole and the DR are strongly coupled. As h is increased to 11 mm, the coupled band is split into two resonant bands. When

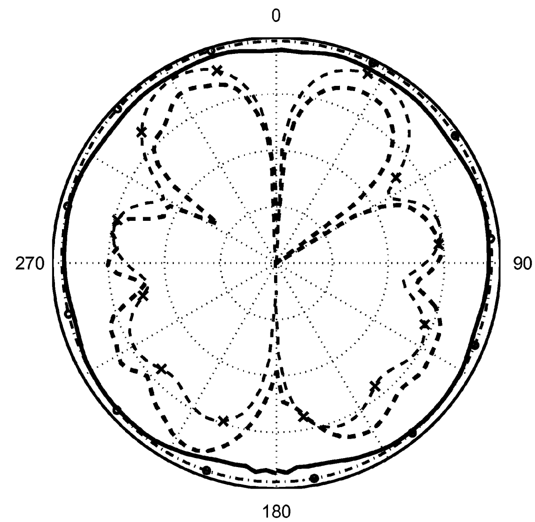

(a)

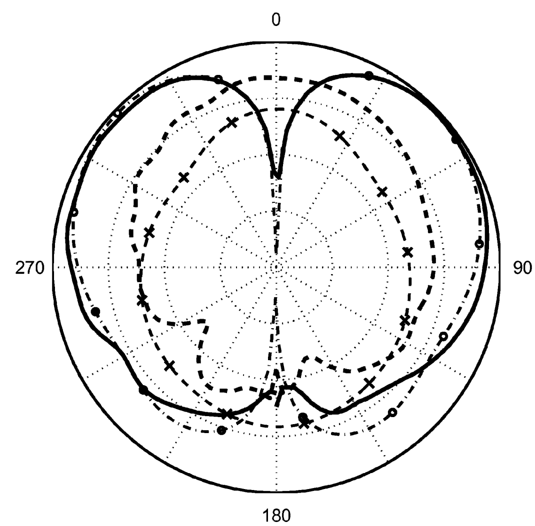

(b)

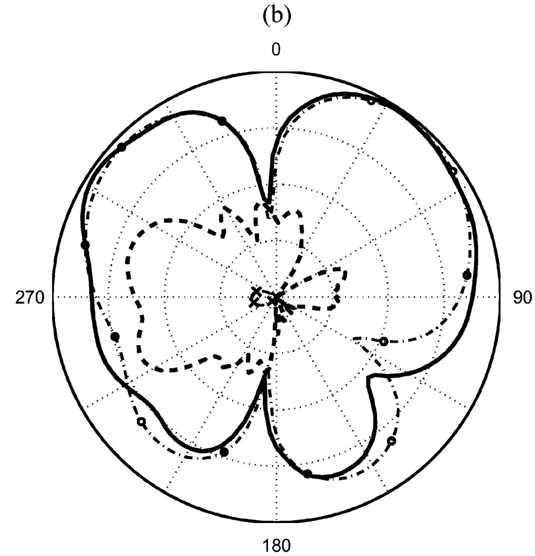

(c)

Fig. 7. Radiation patterns at $f = 4.56$ GHz, (a) xy-plane, (b) yz-plane, (c) xz-plane, —: measured E_θ, - - -: measured E_ϕ, -∘·: simulated E_θ, · × ·: simulated E_ϕ, 10-dB per division on radials, all parameters are the same as in Fig. 5.

h is further increased, the first resonant frequency gradually decreases, and a third null appears between the two nulls associ-

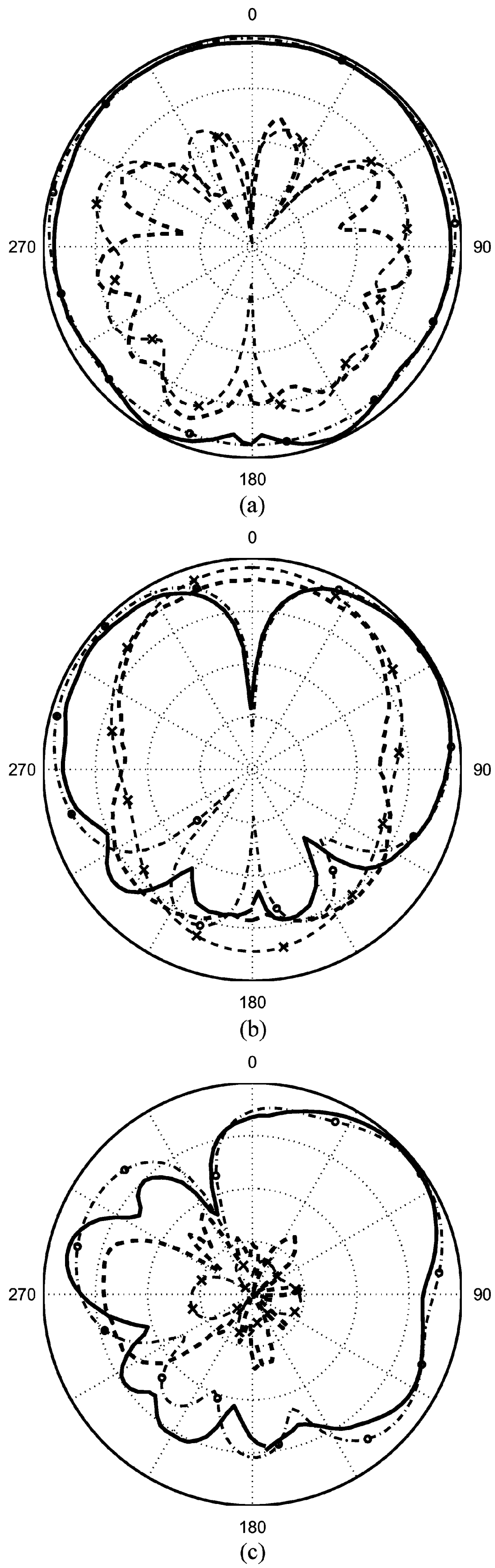

Fig. 8. Radiation patterns at $f = 6.32$ GHz, (a) xy-plane, (b) yz-plane, (c) xz-plane, —: measured E_θ, − − −: measured E_ϕ, −∘·: simulated E_θ, · × ·: simulated E_ϕ, 10-dB per division on radials, all parameters are the same as in Fig. 5.

ated with the monopole mode and the DR mode, respectively. Fig. 10 shows the current distribution and the electric field distribution at $f = 5.5$ GHz, associated with the curve shown in Fig. 9(a) with $h = 13$ mm. The current distribution is similar to that of the DR mode near the bottom and similar to that of the monopole mode around the upper portion.

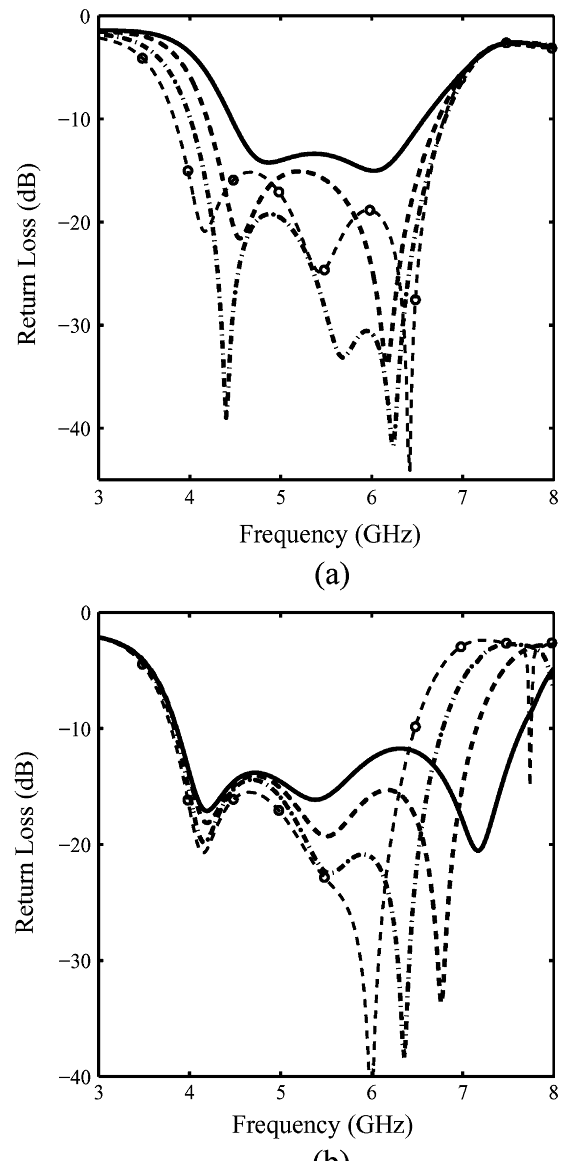

Fig. 9. Effects of antenna height h and dielectric constant on resonant frequency, $a = 3$ mm, $b = 6$ mm, $h_c = 1$ mm, $l = 5.35$ mm, $s = 0.2$ mm, $g = 0.5$ mm, $w = 10$ mm, $W_G = L_G = 70$ mm, $t = 0.6$ mm, (a) $\epsilon_r = 20$, —: $h = 10$ mm, − − −: $h = 11$ mm, −·−: $h = 12$ mm, −∘−: $h = 13$ mm, (b) $h = 12$ mm, —: $\epsilon_r = 16$, − − −: $\epsilon_r = 18$, −·−: $\epsilon_r = 20$, −∘−: $\epsilon_r = 22$.

Fig. 9(b) shows the effect of the DR permittivity on the resonant frequency. As the dielectric constant is increased, the wavelength in the cavity is reduced, rendering a lower resonant frequency. Note that the first resonant frequency is hardly affected by the dielectric constant.

V. Conclusion

In this paper, a broadband CPW-fed DR-monopole is proposed. The resonant bands of monopole and dielectric resonator are coupled to render a wide bandwidth of 47%. The bandwidth can be adjusted by tuning the resonant frequencies of the DR

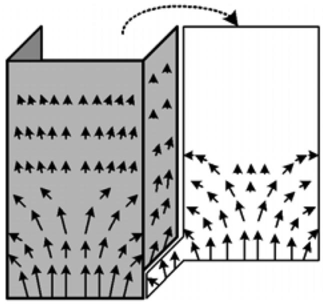

Fig. 10. Current distribution on metal coating (gray surface), and electric field distribution on DR surface (white surface) at $f = 5.5$ GHz, parameters are the same as in Fig. 9(a) with $h = 13$ mm.

and the monopole separately. The E_θ component is nearly omnidirectional on the horizontal plane over the band. The size of the DR-monopole is $12\ \mathrm{mm} \times 3.3\ \mathrm{mm} \times 5.6\ \mathrm{mm}$, and the bandwidth is wide enough to cover the IEEE 802.11a applications.

REFERENCES

[1] A. A. Kishk, B. Ahn, and D. Kajfez, "Broadband stacked dielectric resonator antenna," *Electron. Lett.*, vol. 25, no. 18, pp. 1232–1233, Aug. 1989.

[2] Z. Fan and Y. M. M. Antar, "Slot-coupled DR antenna for dual-frequency operation," *IEEE Trans. Antennas Propag.*, vol. 45, no. 2, pp. 306–308, Feb. 1997.

[3] R. D. Richtmyer, "Dielectric resonators," *J. Appl. Phys.*, vol. 10, pp. 391–398, Jun. 1939.

[4] Y. Y. Hung, "Natural resonant frequencies of microwave dielectric resonators," *IEEE Trans. Microw. Theory Tech.*, vol. 13, pp. 256–256, Mar. 1965.

[5] S. A. Long, M. W. McAllister, and L. C. Shen, "The resonant cylindrical dielectric cavity antenna," *IEEE Trans. Antennas Propag.*, vol. 31, no. 3, pp. 406–412, May 1983.

[6] A. Ittipiboon, A. Petosa, D. Roscoe, and M. Cuhaci, "An investigation of a novel broadband dielectric resonator antenna," in *Proc. IEEE APS Int. Symp.*, Jul. 1996, vol. 3, pp. 2038–2041.

[7] Y.-D. Kim, M.-S. Kim, and H.-M. Lee, "Internal rectangular dielectric resonator antenna with broadband characteristic for IMT-2000 handset," in *Proc. IEEE APS Int. Symp.*, Jun. 2002, vol. 3, pp. 22–25.

[8] A. A. Kishk, "Wide-band truncated tetrahedron dielectric resonator antenna excited by a coaxial probe," *IEEE Trans. Antennas Propag.*, vol. 51, no. 10, pp. 2913–2917, Oct. 2003.

[9] A. A. Kishk, Y. Yan, and A. W. Glisson, "Conical dielectric resonator antennas for wide-band applications," *IEEE Trans. Antennas Propag.*, vol. 50, no. 5, pp. 469–474, Apr. 2002.

[10] R. K. Mongia, A. Ittibipoon, and M. Cuhaci, "Low profile dielectric resonator antennas using a very high permittivity material," *Electron. Lett.*, vol. 30, no. 17, pp. 1362–1363, Aug. 1994.

[11] K. W. Leung, K. M. Chow, and K. M. Luk, "Low-profile high-permittivity dielectric resonator antenna excited by a disk-loaded coaxial aperture," *IEEE Antennas Wireless Propag. Lett.*, vol. 2, pp. 212–214, 2003.

[12] F. R. Hsiao, C. Wang, K. L. Wong, and T. W. Chiou, "Broadband very-high-permittivity dielectric resonator antenna for WLAN application," in *Proc. IEEE APS Int. Symp.*, Jun. 2002, vol. 4, pp. 490–493.

[13] A. Buerkle, K. Sarabandi, and H. Mosallaei, "Compact slot and dielectric resonator antenna with dual-resonance, broadband characteristics," *IEEE Trans. Antennas Propag.*, vol. 53, no. 3, pp. 1020–1027, Mar. 2005.

[14] K. P. Esselle and T. S. Bird, "A hybrid-resonator antenna: Experimental results," *IEEE Trans. Antennas Propag.*, vol. 53, no. 2, pp. 870–871, Feb. 2005.

[15] T. A. Denidni and Q. Rao, "Hybrid dielectric resonator antennas with radiating slot for dual-frequency operation," *IEEE Antennas Wireless Propag. Lett.*, vol. 3, pp. 321–323, 2004.

[16] K. Lan, S. K. Chaudhuri, and S. S. Naeini, "Design and analysis of a combination antenna with rectangular dielectric resonator and inverted L-plate," *IEEE Trans. Antennas Propag.*, vol. 53, no. 1, pp. 495–501, Jan. 2005.

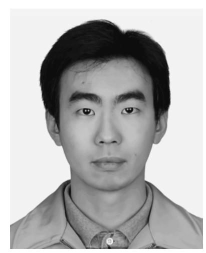

Tze-Hsuan Chang (S'00) was born in Hsin-Chu, Taiwan, R.O.C., on February 1, 1978. He received the B.S. degree in electrical engineering from the National Chung Hsing University, Taiwan, R.O.C., in July 2000. Currently, he is working towards the Ph.D. degree in the Graduate Institute of Communication Engineering, National Taiwan University, Taipei, Taiwan, R.O.C.

Jean-Fu Kiang (M'89) was born in Taipei, Taiwan, R.O.C., on February 2, 1957. He received the B.S. and M.S. degrees from National Taiwan University, Taiwan, R.O.C., and the Ph.D. degree from the Massachusetts Institute of Technology, Cambridge, in 1979, 1981, and 1989, respectively, all in electrical engineering.

From 1985 to 1986, he was with Schlumberger-Doll Research, Ridgefield, CT; from 1989 to 1990, IBM Watson Research Center, Yorktown Heights, NY; from 1990 to 1992, Bellcore, Red Bank, NJ; from 1992 to 1994, Siemens Electromedical Systems, Danvers, MA; and from 1994 to 1999, National Chung-Hsing University, Taichung, Taiwan, R.O.C. Since 1999, he has been a Professor in the Department of Electrical Engineering and the Graduate Institute of Communication Engineering, National Taiwan University. His research interests include the applications and system issues on electromagnetics, wireless communications, antennas, electromagnetic compatibility, microwave components, etc.